Dasatinib suppresses atherosclerotic lesions by suppressing cholesterol uptake in a mouse model of hypercholesterolemia

Journal of Pharmacological Sciences 149 (2022) 158–165

Contents lists available at ScienceDirect

Journal of Pharmacological Sciences

journal homepage: www.elsevier.com/locate/jphs

Full Paper

Dasatinib suppresses atherosclerotic lesions by suppressing cholesterol uptake in a mouse model of hypercholesterolemia

Masamitsu Takaba [a], Takayuki Iwaki [b,*], Tomohiro Arakawa [b], Takaaki Ono [a], Yuichiro Maekawa [a], Kazuo Umemura [b]

[a] Third Division, Department of Internal Medicine, Hamamatsu University School of Medicine, 1-20-1 Handayama, Higashi-ku, Hamamatsu, 431-3192, Japan
[b] Department of Pharmacology, Hamamatsu University School of Medicine, 1-20-1 Handayama, Higashi-ku, Hamamatsu, 431-3192, Japan

ARTICLE INFO

Article history:
Received 24 November 2021
Received in revised form
24 March 2022
Accepted 21 April 2022
Available online 7 May 2022

Keywords:
Atherosclerosis
Cardiovascular event
Cd36
Dasatinib
Sortilin

ABSTRACT

Although the use of BCR-ABL1 tyrosine kinase inhibitors (TKIs) for chronic myeloid leukemia is known to cause vascular adverse events (VAEs), the frequency of VAEs during dasatinib administration is not high, and the same holds for atherosclerosis-related VAEs. However, its effect on atherosclerosis remains controversial. In this study, our primary objective was to investigate how dasatinib affects atherosclerosis. *Ldlr*$^{-/-}$/*Apobec1*$^{-/-}$ mice, which are highly prone to develop atherosclerosis, were administered dasatinib. After 16 weeks, we evaluated their atherosclerotic lesions. We used bone-marrow-derived macrophages to investigate the uptake of oxidized low-density lipoprotein (LDL) complexed with DiI dye (DiI-oxLDL). RNA sequencing and quantitative reverse transcription polymerase chain reaction (RT-qPCR) were performed to explore the potential effects of dasatinib on cholesterol metabolism. Dasatinib administration significantly reduced atherosclerotic lesions ($P < 0.001$ and $P = 0.013$) and DiI-oxLDL uptake ($P < 0.001$) unlike other TKIs. RNA sequencing and RT-qPCR suggested that *Sort1*, which encodes sortilin, a known regulator of LDL uptake, and *Cd36* were potential targets of dasatinib. In conclusion, dasatinib induced elevated LDL-C levels, but oxLDL uptake in macrophages were suppressed, resulting in reducing atherosclerotic lesions. These results further our understanding of the differences in VAEs between dasatinib and other TKIs.

1. Introduction

Clinical outcomes in chronic myeloid leukemia (CML) have substantially improved with the introduction of BCR-ABL1 tyrosine kinase inhibitors (TKIs).[1] Consequently, TKI-administered patients with chronic-phase CML have a life expectancy similar to that of age-matched subjects.[2] Nonetheless, most patients with chronic-phase CML cannot discontinue TKIs for the rest of their lives.

Nilotinib and dasatinib, second-generation TKIs, have a greater effect on the BCR-ABL1 fusion gene than imatinib, the first-generation TKI.[3,4] Ponatinib, a third-generation TKI, affects CML via the TKI-refractory threonine-to-isoleucine mutation at position 315 (T315I).[5] These TKIs yield improved treatment outcomes in patients with CML. However, recent reports have shown that the long-term administration of second- or third-generation TKIs increases the incidence of vascular adverse events (VAEs), which can be life-threatening.[6–10] This is considered to be due to the off-target effects of BCR-ABL1 TKIs because the adverse–effect profile and the frequency of VAEs differ among TKIs. In the clinical setting, where most patients with CML require long-term TKI administration, the unique VAEs must be carefully managed during each TKI administration.[11]

Interestingly, dasatinib is associated with a different VAE profile compared with other TKIs. The frequency of VAEs during dasatinib administration is not high.[4,6,12] Atherosclerosis-related VAEs such as myocardial infarction and stroke are common during nilotinib and ponatinib administration, although their incidence does not increase to the same degree during dasatinib administration.[6] The main reasons are considered to be the different characteristics of dasatinib compared with other TKIs. Dasatinib has over 50 tyrosine kinase targets, which considerably exceeds the number of targets of

* Corresponding author. Fax: +81 53 435 2271; +81 53 435 2269.
E-mail address: tiwaki@hama-med.ac.jp (T. Iwaki).
Peer review under responsibility of Japanese Pharmacological Society.

https://doi.org/10.1016/j.jphs.2022.04.009

other TKIs.[13] Although details of the underlying mechanism remain unclear, the difference may result in different frequencies of atherosclerosis-related VAEs.

Several studies have reported the mechanisms underlying TKI-related VAEs. For instance, aspects investigated include the involvement of interleukin (IL)-1β in the vascular endothelium,[14] anti-angiogenic blocking of vascular endothelial growth factor receptor in vascular endothelial cells,[15] adverse effects on human vascular function,[16] and cardiovascular toxicity due to thrombotic microangiopathy.[17] In particular, several studies using *Apoe*$^{-/-}$ mice or APOE*3Leiden.CETP mice have revealed the relationship between imatinib, nilotinib, and ponatinib administration and atherosclerosis.[18,19] However, despite the interesting suggestion that the frequency of atherosclerosis-related VAEs is not high during dasatinib administration, the association between dasatinib and atherosclerotic lesions has never been studied in an atherosclerotic mouse model. In addition, these studies have reported inconsistent findings regarding atherosclerotic lesion production with imatinib and nilotinib administration. Moreover, although atherosclerosis-related VAEs are often observed during ponatinib administration in patients with CML, ponatinib reduced plasma cholesterol level and prevented atherosclerosis lesion progression in APOE*3Leiden.CETP mice.[19] These studies have revealed that these TKIs affect the vascular endothelial cells and coagulatory systems. However, their mechanisms related to atherosclerosis remain unclear. Therefore, we examined the relationships between dasatinib and atherosclerosis using *Ldlr*$^{-/-}$/*Apobec1*$^{-/-}$ mice. *Ldlr*$^{-/-}$/*Apobec1*$^{-/-}$ mice have high plasma low-density lipoprotein (LDL) levels and a more pronounced development of atherosclerosis when fed a normal diet, whereas *Apoe*$^{-/-}$ mice are characterized by elevated levels of intermediate-density lipoprotein (IDL) and very-low-density lipoprotein (VLDL) on a high-fat diet.[20]

The primary objective of this study was to investigate the mechanisms of dasatinib on atherosclerosis. The present study provides new insights into the relationships between TKIs and atherosclerosis.

2. Materials and methods

2.1. Drugs

For comparison with dasatinib, we evaluated imatinib and nilotinib in some of the experiments. Imatinib was obtained from Tokyo Chemical Industry (Tokyo, Japan). Nilotinib and dasatinib were obtained from ChemScene (Monmouth Junction, NJ). These TKIs were diluted with dimethyl sulfoxide (DMSO) (Sigma–Aldrich, St. Louis, MO). DMSO was used as the vehicle control.

2.2. Evaluation of atherosclerotic lesions and plasma cholesterol levels in *Ldlr*$^{-/-}$/*Apobec1*$^{-/-}$ mice

Ldlr$^{-/-}$/*Apobec1*$^{-/-}$ mice were back-crossed with C57Bl6/J mice (Jackson Laboratory, Bar Harbor, ME) for at least seven generations before cross-breeding. Eight-week-old male *Ldlr*$^{-/-}$/*Apobec1*$^{-/-}$ mice were randomized in four groups as follows: control (n = 11), administered 200 μL of DMSO as the vehicle control; imatinib (n = 10), administered imatinib (50 mg/kg/day); nilotinib (n = 11), administered nilotinib (45 mg/kg/day); and dasatinib (n = 10), administered dasatinib (50 mg/kg/day). The dose settings of TKIs were quoted from the monograph for each TKI. These TKIs were diluted with 200 μL of DMSO. The drugs were administered via oral gavage for 16 cycles in total, with one cycle lasting a week with 2 consecutive days off and 5 consecutive days of administration. The mice were sacrificed by isoflurane overdose (Pfizer, New York City, NY). Their blood was then collected in a tube containing sodium citrate. The heart, aorta, and liver samples were obtained after perfusion in saline. The heart and aorta samples were evaluated for atherosclerotic lesions, and the liver samples were stored at −80 °C until use. All animal experiments were approved by the Animal Care and Use Committee of Hamamatsu University School of Medicine and were performed according to the guidelines of this committee.

2.3. Histopathology

The hearts were quickly removed, fixed in 10% buffered formalin (Kanto Chemical Co., Inc., Tokyo, Japan), and embedded in paraffin. Subsequently, 3-μm-thick heart sections containing the aortic root with valve leaflets were stained with hematoxylin–eosin and Masson's trichrome stain to evaluate atherosclerotic lesions. These sections were scanned and observed using a BX53 microscope (Olympus, Tokyo, Japan). The atherosclerotic lesion area was measured using ImageJ.[21] The percentage of atherosclerotic lesions in the aortic root sections was assessed by dividing the atherosclerotic lesion area by the entire aortic root area.

The aortas were cut longitudinally and fixed in 10% buffered formalin. After rinsing with phosphate-buffered saline (PBS) and 70% ethanol, the aorta sections were stained with Sudan IV (Sigma–Aldrich) and photographed using a digital camera (Nikon D7200; Nikon Corporation, Tokyo, Japan). The atherosclerotic lesion area was measured using ImageJ.[20] The atherosclerotic lesion percentage in the aortic atherosclerosis was assessed by dividing the atherosclerotic lesion area by the entire aortic area.

2.4. Plasma cholesterol analysis

Blood samples were collected from the inferior vena cava at the time of sacrifice and placed into sodium citrate-containing tubes. After centrifuging, the plasma was stored at −80 °C until use. Plasma total cholesterol (TC), LDL-C, and high-density lipoprotein-cholesterol (HDL-C) levels were measured using a direct assay by Oriental Yeast Co., Ltd (Tokyo, Japan).

2.5. Cell culture

We used bone-marrow-derived macrophages. Bone marrow cells were collected from the femurs of male 8-week-old *Ldlr*$^{-/-}$/*Apobec1*$^{-/-}$ mice. These cells were cultured in RPMI-1640 (FUJIFILM Wako Pure Chemical Corporation, Osaka, Japan) supplemented with 20% fetal bovine serum (Life Technologies, Carlsbad, CA), 20 ng/mL macrophage colony-stimulating factor (FUJIFILM Wako Pure Chemical Corporation), and antibiotic/antimycotic solution (100 U/mL penicillin G, 100 μg/mL streptomycin, and 250 ng/mL amphotericin B) (FUJIFILM Wako Pure Chemical Corporation) for 7 days. Finally, bone-marrow-derived macrophages were collected using Accumax (Innovative Cell Technologies, San Diego, CA) and used to measure DiI-oxLDL uptake.

2.6. Measurement of DiI-oxLDL uptake by bone-marrow-derived macrophages under TKI administration

Bone-marrow-derived macrophages were resuspended (5.0×10^6 cells/mL), and 100 μL of cell suspension was placed into each well of a 96-well plate with DMSO as the vehicle control, imatinib (1000 nmol/L), nilotinib (1000 nmol/L), or dasatinib (100 nmol/L) for 24 h. These concentrations were based on visual observation of cells subjected to trypan blue staining following each TKI administration (Fig. S1). The researchers who analyzed cell proliferation were blinded to TKI administration to curtail bias. We eliminated the effect of cell proliferation on reduced uptake by normalizing the rate of cell proliferation. After incubation with these

TKIs, the cells were incubated with oxidized LDL complexed with DiI dye (DiI-oxLDL) (Life Technologies) for 3 h and washed with PBS according to the manufacturer's instructions. The cells were photographed using Celldiscoverer 7 (Carl Zeiss, Jena, Germany). The fluorescence intensity at 592 nm was analyzed using ImageJ.

2.7. RNA sequencing

To further study the mechanism underlying the reduction of atherosclerotic lesions and cholesterol uptake suppression during long-term dasatinib administration, RNA sequencing was conducted in mice treated with long-term dasatinib or vehicle. The total RNA was extracted from the mice livers using the RNeasy Mini Kit (Qiagen, Valencia, CA) according to the manufacturer's instructions. The total RNA quality was checked using NanoDrop 1000 (Thermo Fisher Scientific, Waltham, MA), and the RNA integrity of the samples was assessed. All samples cleared the quality checks. Libraries were constructed using a TruSeq Stranded mRNA LT Sample Prep Kit (Illumina, San Diego, CA) and sequenced on the Illumina platform. Raw data were trimmed using Trimmomatic 0.38 (http://www.usadellab.org/cms/?page=trimmomatic). Trimmed data were mapped to a reference genome (mm10) using HISAT2 v. 2.1.0 and Bowtie2 v. 2.3.4.1 (ccb.jhu.edu/software/hisat2/index.shtml). Differentially expressed genes (DEGs) were identified using StringTie v. 2.1.3b (ccb.jhu.edu/software/stringtie/). The significance threshold was $P < 0.05$, and fold change of >2 or <0.5 was used to identify DEGs. These processes were supported by Macrogen Japan Corp. (Tokyo, Japan).

2.8. Western blotting

The expression of proteins was evaluated by western blotting to confirm the results obtained from RNA sequencing. Liver lysates were prepared by placing liver homogenates in Cell Lysis Buffer (FUJIFILM Wako Pure Chemical Corporation) containing protease inhibitors. The supernatant after centrifugation was used for SDS-polyacrylamide gel electrophoresis and immunoblotting. We used antibodies specific to β-actin (66009-1-Ig; Proteintech, Rosemont, IL) and sortilin (EPR23093-58; Abcam plc, Cambridge, UK) according to the manufacturers' instructions. Anti-β-actin and anti-sortilin antibodies were diluted to 1/20,000 using 5% skim milk and 1/1000 using tris(hydroxymethyl)aminomethane-buffered saline with Tween 20 (TBS-T), respectively. We used anti-mouse IgG (H + L), horseradish peroxidase (HRP)-linked (074–1806; Kirkegaard & Perry Laboratories, Inc., Gaithersburg, MD), and anti-rabbit IgG, HRP-linked antibodies (7074S; Cell Signaling Technology, Danvers, MA) as secondary antibodies for β-actin and sortilin, respectively. Both secondary antibodies were diluted to 1/4000 using TBS-T. Protein bands were visualized using Amersham ECL Prime reagent (Cytiva, Tokyo, Japan) and analyzed using GelAnalyzer v. 2010a freeware (www.gelanalyzer.com). β-Actin was used as an internal control, and sortilin band intensity was normalized to β-actin intensity.

2.9. Quantitative reverse transcription polymerase chain reaction (RT-qPCR)

To examine the expression of *Sort1*, *Cd36* and *Msr1* mRNA, reverse transcription was performed using a ReverTra Ace qPCR RT Master Mix with gDNA Remover (TOYOBO, Tokyo, Japan). The total RNA was extracted from livers and peritoneal macrophages using the RNeasy Mini Kit (Qiagen, Valencia, CA) according to the manufacturer's instructions. RT-qPCR was performed using the THUNDERBIRD SYBR qPCR Mix (TOYOBO) and QuantStudio 3 (Thermo Fisher Scientific). The *Sort1* primer sequences were 5′-ACTTCACTGGGCTTGCTTCC-3` (forward) and 5′-CCTCTTCACAATTCCGCTCA-3` (reverse). The *Cd36* and *Msr1* primer sequences were 5′-CAAAACGACTGCAGGTCAAC-3` (forward) and 5′-CCAATGGTCCCAGTCTCATT-3` (reverse) and 5′-GGAATAAGAGGTATTCCAGGT-3` (forward) and 5′-TTTGTCCTTTAGGTCCAGGAC-3` (reverse), respectively. The relative target gene transcript levels were standardized to that of 18S rRNA and are expressed as fold changes derived from the ΔΔCt values. The 18S rRNA primer sequences were 5′-GGTAACCCGTTGAACCCCATT-3` (forward) and 5′-CAACGCAAGCTTATGACCCG-3` (reverse). All primers were provided by Eurofins Genomics (Tokyo, Japan).

2.10. Evaluation of mRNA expression in peritoneal macrophages under dasatinib administration

Peritoneal macrophages were collected from 24-week-old male *Ldlr*$^{-/-}$/*Apobec1*$^{-/-}$ mice. First, 3% thioglycolate (BD Biosciences, Franklin Lakes, NJ) was injected intraperitoneally. Four days after the injection, peritoneal cells were collected from the peritoneal cavity using PBS. These cells were cultured in RPMI-1640 supplemented with 20% fetal bovine serum and antibiotic/antimycotic solution (100 U/mL penicillin G, 100 μg/mL streptomycin, and 250 ng/mL amphotericin B) for 1.5 h in the cell culture dish. After washing twice with PBS, the adherent cells were considered peritoneal macrophages. Peritoneal macrophage suspension was placed equally into each well of a 6-well plate with DMSO or dasatinib (100 nmol/L) for 24 h. The number in each group was as follows: control (n = 6) and dasatinib (n = 6). After incubation, the total RNA was extracted from these samples and RT-qPCR was conducted.

We further evaluated the effect of dasatinib on peritoneal macrophages after oral gavage. The number of mice in each group was as follows: control (n = 8) and dasatinib (n = 8). First, DMSO or dasatinib (50 mg/kg/day) were administered via oral gavage for 7 days. Second, 3% thioglycolate was injected intraperitoneally on the third day of administration. Third, peritoneal macrophages were collected on the seventh day of administration. The total RNA was extracted from these samples and RT-qPCR was conducted.

2.11. Statistical analysis

Differences between two groups were compared using the *t*-test. For multiple group comparisons, a one-way ANOVA followed by Dunnett's test was performed. The significance threshold was $P < 0.05$. All statistical analyses were conducted using GraphPad Prism v. 8.10 for Windows (GraphPad Software, La Jolla, CA).

2.12. Data availability

The data supporting the findings of this study are available from the corresponding author upon reasonable request.

3. Results

3.1. Dasatinib reduced plaque lesions in the aortic root sinus and aorta

First, we evaluated plaque lesions in the aortic root sinus. Few plaque lesions were observed in the dasatinib group (Fig. 1A), which had significantly smaller lesions than the control group (−146%, $P < 0.001$; Fig. 1B). While there was a significant reduction in response to treatment with dasatinib, the total area of plaque lesions did not significantly change among the groups treated with imatinib, nilotinib, and the control. Owing to technical issues, the number of specimens obtained from each group was as follows: control (n = 10), imatinib (n = 10), nilotinib (n = 11), and dasatinib (n = 9).

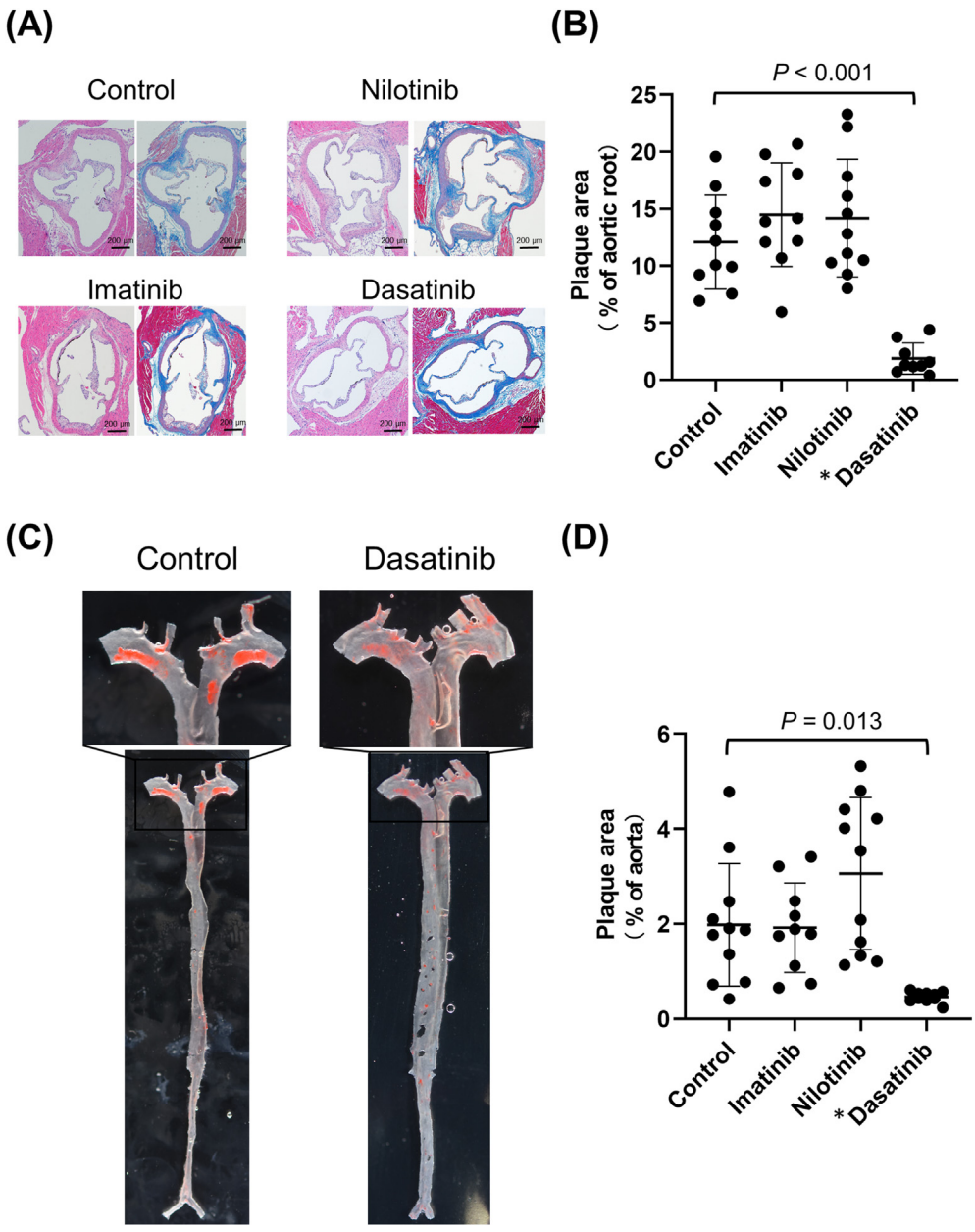

Fig. 1. Effects of BCR/ABL1 tyrosine kinase inhibitors on atherosclerotic lesions. (A) Aortic root section. The images were captured using a BX53 microscope; scale bar = 200 μm. Representative images of hematoxylin–eosin (left) and Masson's trichrome (right) staining for atherosclerosis of the aortic root in the control, imatinib, nilotinib, and dasatinib groups. (B) Aortic root lesion area measured using ImageJ. The lesions were significantly smaller in the dasatinib group than in the control (−146%, $P < 0.001$). However, there was no difference between the control and non-dasatinib groups. The number of mice in each group was as follows: control (n = 10), imatinib (n = 10), nilotinib (n = 11), and dasatinib (n = 9). (C) Aortic atherosclerosis samples stained with Sudan IV. The images were captured using a digital camera (Nikon D7200). (D) Size of aortic lesions measured using ImageJ. The lesions were also significantly smaller in the dasatinib group than in the control group (−124%, $P = 0.013$). In contrast, there was no significant difference between the control and non-dasatinib groups. The number of mice in each group was as follows: control (n = 11), imatinib (n = 10), nilotinib (n = 11), and dasatinib (n = 10). The single asterisk (*) indicates a statistically significant difference from control by $P < 0.05$.

Second, we evaluated the plaque lesions in aortic atherosclerosis (Fig. 1C) and observed a significant reduction following treatment with dasatinib compared with that in the control; these results were consistent with those for the aortic root sinus lesions (−124%, $P = 0.013$; Fig. 1D).

3.2. Dasatinib increased the TC and LDL-C levels

The TC and LDL-C levels were higher in the dasatinib group than in the control ($P = 0.017$ and $P = 0.023$, respectively; Fig. 2). In the imatinib and nilotinib groups, the TC and LDL-C levels did not differ from those in the control. The HDL-C level did not differ between any of the TKI groups and the control.

3.3. Dasatinib suppressed DiI-oxLDL uptake in bone-marrow-derived macrophages

To assess cholesterol uptake under each TKI administration, we assessed oxLDL uptake using DiI-oxLDL. DiI-oxLDL uptake by bone-marrow-derived macrophages was significantly lower in the dasatinib group than in the vehicle group ($P < 0.001$; Fig. 3). Dasatinib was more effective than the other TKIs in reducing

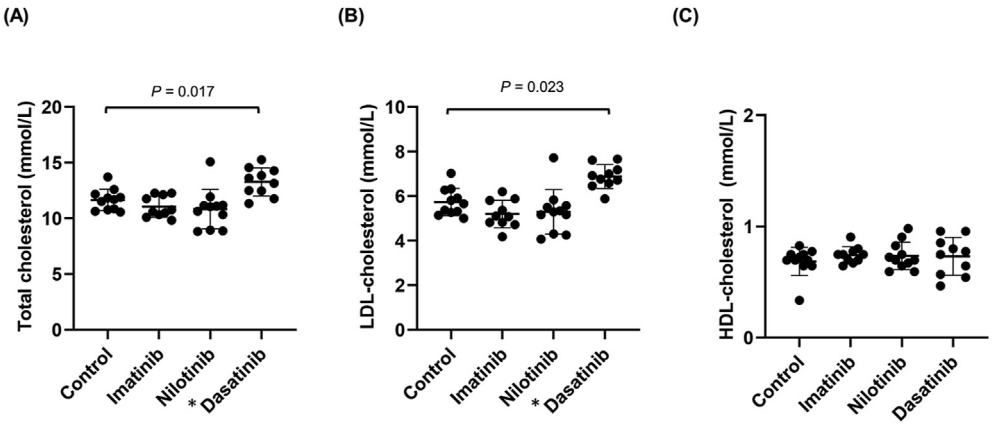

Fig. 2. TC, LDL-C, and HDL-C levels in each group. (A) The TC level was higher in the dasatinib group than in the control group ($P = 0.017$). In contrast, the TC level did not differ among the control, imatinib, and nilotinib groups. (B) The LDL-C level was higher in the dasatinib group than in the control group ($P = 0.023$). In contrast, the LDL level did not differ among the control, imatinib, and nilotinib groups. (C) The HDL-C level did not differ between any of the TKI groups and the control. The number of mice in each group was as follows: control (n = 11), imatinib (n = 10), nilotinib (n = 11), and dasatinib (n = 10). The single asterisk (*) indicates a statistically significant difference from control by $P < 0.05$. TC: total cholesterol, LDL-C: low-density lipoprotein cholesterol, HDL: high-density lipoprotein cholesterol.

cholesterol uptake. In contrast, there was no difference among the control, imatinib administration, and nilotinib groups in terms of cholesterol uptake.

3.4. RNA sequencing

In total, 752 DEGs were identified using the specified selection criteria ($P < 0.05$; fold change >2 or < 0.5). Among these, the expression of 387 DEGs was upregulated, whereas that of 365 DEGs was downregulated compared with the control levels (Table S1). We compared the dasatinib and control groups via a hierarchical clustering heat map and volcano map of DEGs (Fig. S2). Although hierarchical clustering heat maps revealed similar DEG patterns between the dasatinib and control groups, different DEG patterns were observed between them (Fig. S2A). The volcano map showed similar numbers of upregulated and downregulated DEGs (Fig. S2B). These results suggested that the expression of *Sort1*, which encodes sortilin, was lower in the dasatinib group than in the control group.

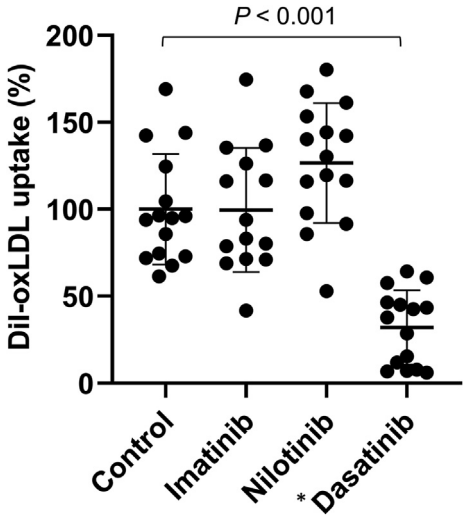

Fig. 3. Dil-oxLDL uptake by bone-marrow-derived macrophages exposed to different BCR/ABL1 tyrosine kinase inhibitors. Dil-oxLDL uptake by the bone-marrow-derived macrophages was significantly lower in the dasatinib group compared with that in the control ($P < 0.001$), and it was the lowest in the dasatinib group. Dil-oxLDL uptake did not differ among the control, imatinib, and nilotinib groups. The single asterisk (*) indicates a statistically significant difference from control by $P < 0.05$. Dil-oxLDL: oxidized low-density lipoprotein complexed with Dil dye.

3.5. Dasatinib suppressed the expression of sortilin protein and Sort1 mRNA in the liver

To confirm the expression of sortilin, we performed western blotting. The number of samples including the RNA sequencing samples was as follows: control (n = 6), imatinib (n = 5), nilotinib (n = 6), and dasatinib (n = 6). Western blotting revealed lower sortilin expression in the dasatinib group than in the control ($P = 0.006$; Fig. 4A). In the imatinib and nilotinib groups, the sortilin level did not differ from that in the control. These results support that dasatinib treatment also suppressed the expression of sortilin.

We further conducted RT-qPCR to investigate the expression of *Sort1*, *Cd36*, and *Msr1* mRNA in the liver. The number of samples including the RNA sequencing samples was as follows: control (n = 6) and dasatinib (n = 6). RT-qPCR revealed lower *Sort1* expression in the dasatinib-treated group than in the control ($P = 0.041$; Fig. 4B). In contrast, *Cd36* mRNA expression was higher in the dasatinib-treated group than in the control group ($P = 0.002$; Fig. 4B). The expression of *Msr1* mRNA was not detectable (data not shown).

3.6. Dasatinib suppressed the expression of Cd36 mRNA in peritoneal macrophages

We also conducted RT-qPCR using total RNA from peritoneal macrophages and explored the effect of dasatinib on macrophages. These results revealed that *Cd36* expression was lower in the dasatinib administration than in the control after incubation ($P = 0.001$; Fig. 4C) and oral gavage ($P < 0.001$; Fig. 4D). In contrast, *Sort1* expression in dasatinib administration had no significant changes after incubation ($P = 0.38$; Fig. 4C) and oral gavage ($P = 0.93$; Fig. 4D).

4. Discussion

In this study, we evaluated atherosclerotic lesions with TKI administration in *Ldlr*$^{-/-}$/*Apobec1*$^{-/-}$ mice. Dasatinib administration significantly reduced the atherosclerotic lesions compared

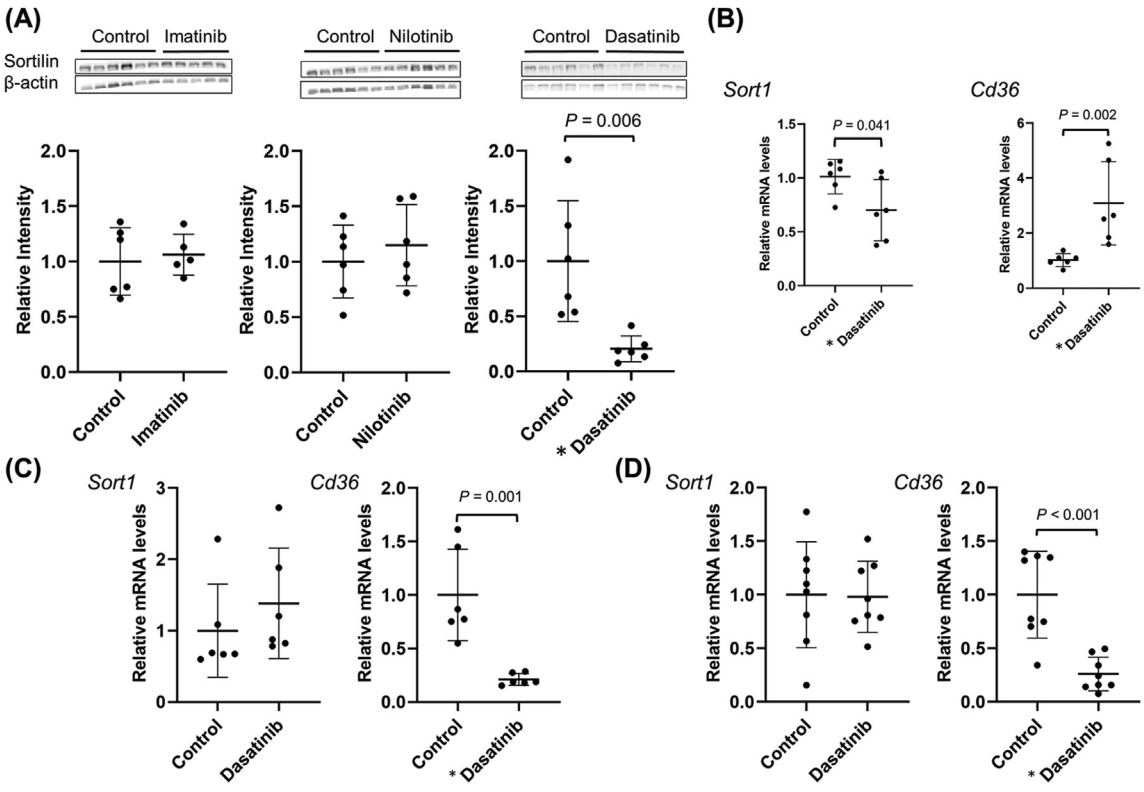

Fig. 4. Relative expression of sortilin protein, *Sort1* mRNA, and *Cd36* mRNA. (A) The relative expression of sortilin protein in livers. The expression of sortilin, detected by western blotting, was lower in the dasatinib-treated group than in the control group ($P = 0.006$). In contrast, sortilin expression did not differ between the control and imatinib groups, and between the control and nilotinib groups. The number of mice in each group was as follows: control (n = 6), imatinib (n = 5), nilotinib (n = 6), and dasatinib (n = 6). (B) The relative expression of *Sort1* and *Cd36* mRNA in livers. *Sort1* mRNA expression, detected using RT-qPCR, was lower in the dasatinib-treated group than in the control group ($P = 0.041$). In contrast, *Cd36* mRNA expression was higher in the dasatinib-treated group than in the control group ($P = 0.002$). The number of mice in each group was as follows: control (n = 6) and dasatinib (n = 6). (C) The relative expression of *Sort1* and *Cd36* mRNA in peritoneal macrophages after incubation. *Sort1* mRNA expression in dasatinib administration had no significant changes after incubation ($P = 0.38$). In contrast, *Cd36* mRNA expression was lower in the dasatinib administration than in the control after incubation ($P = 0.001$). (D) The relative expression of *Sort1* and *Cd36* mRNA in peritoneal macrophages after oral gavage. *Sort1* mRNA expression in dasatinib administration had no significant changes after oral gavage ($P = 0.93$). However, *Cd36* mRNA expression was lower in the dasatinib administration than in the control after oral gavage ($P < 0.001$). The number of mice in each group was as follows: control (n = 8) and dasatinib (n = 8). The single asterisk (*) indicates a statistically significant difference from control by $P < 0.05$.

with the control and other TKI-administered groups. This result showed that dasatinib exerts an atheroprotective effect in this murine model. We then assessed oxLDL uptake by macrophages using DiI-oxLDL. The results showed that dasatinib was more effective than the other TKIs in reducing cholesterol uptake. These findings suggest that the reduction in oxLDL uptake by macrophages with dasatinib administration may inhibit the development of plaque lesions.

Several studies have reported various effects of dasatinib on macrophages.[22,23] For examples, anti-inflammatory effect has been described as a change in macrophage polarization toward the M2 phenotype, which expresses anti-inflammatory cytokines such as interleukin (IL)-10, and is involved in inflammation control and tissue repair after inflammation.[22] In addition, anti-inflammatory and anti-fibrotic effects of dasatinib via the reduction of infiltration of macrophages have been described.[23] Our study also showed a significant reduction in oxLDL uptake by macrophages under dasatinib administration. Therefore, it is possible that the mechanism of dasatinib involves multiple factors associated with atherosclerosis besides the reduction in oxLDL uptake via the effect on macrophages.

We conducted RNA sequencing using liver samples to explore the effects of dasatinib on cholesterol metabolism, and *Sort1* was identified as one of the targets. We then confirmed that dasatinib suppressed sortilin expression unlike other TKIs. *Sort1* is expressed ubiquitously, for example, in neurons, hepatocytes, and white blood cells, including macrophages.[24] Sortilin has various functions, among which, the main one is protein transport. It can act as a multiligand receptor with functions that include LDL uptake in the liver, macrophages in vessel walls,[25] and various other cells.[26] The overexpression of sortilin increases cell surface binding and LDL internalization.[27] *Sort1* expression in macrophages promotes atherosclerosis,[25–29] and sortilin deficiency in mice protects against atherosclerosis by reducing macrophage LDL uptake.[25] Therefore, it is possible that one of the potential effects of dasatinib on cholesterol metabolism could be affected via hepatic sortilin. However, the relationship between *Sort1* and dasatinib has not been reported so far and future studies are required to identify the kinase targets.

Cd36 and *Msr1*, scavenger receptors which play an important role in the uptake of oxLDL, showed no significant findings in RNA sequencing using the specified selection criteria. However, *Cd36* expression was increased by dasatinib administration in livers. *Msr1* mRNA expression was not detectable. These results showed that dasatinib affected various factors including *Cd36* because it has a significant number of kinase targets. The reason for the increased expression of *Cd36* in livers remains unclear. In contrast, the decreased expression of *Cd36* under dasatinib administration was observed in peritoneal macrophages unlike livers. *Sort1* expression under dasatinib administration had no significant

changes. Taken together, dasatinib may have potential effects on atherosclerotic lesions by reducing cholesterol uptake via *Cd36* in macrophages.

Atherosclerotic lesions generally exacerbate when plasma cholesterol levels increase. However, dasatinib attenuated the atherosclerotic lesions, although the TC and LDL-C levels were higher in the dasatinib group than in the control. The relationships between plasma cholesterol levels and sortilin are inconsistent and controversial because hepatic sortilin plays an important role in both cholesterol uptake and secretion. Some studies have reported that *Sort1* deficiency reduces plasma cholesterol levels in both western diet-fed *Ldlr*$^{-/-}$ mice and western diet-fed wild type mice.[28,30] However, elevated plasma LDL-C levels were observed with *Sort1* knockdown in *Apobec1*$^{-/-}$ mice.[31] In contrast, *Cd36* deficiency increases plasma cholesterol levels in western diet-fed *Apoe*$^{-/-}$ mice.[32] In our study, dasatinib administration decreased hepatic sortilin and increased *Cd36* expression in the liver but attenuated it in peritoneal macrophages. Therefore, the increased plasma cholesterol levels in our model were attributed to be the results of the complex function of various factors in each organ. Suppression of atherosclerotic lesions was thought to be mainly due to the reduction in cholesterol uptake of macrophages rather than the involvement of plasma cholesterol levels.

In conclusion, our study demonstrated that dasatinib induced elevated LDL-C levels, but oxLDL uptake in macrophages were suppressed, resulting in reducing atherosclerotic lesions in a mouse model of hypercholesterolemia. Our findings regarding the effects of dasatinib provide new insights into the relationships between TKIs and atherosclerosis.

Author contributions

All authors contributed to the design of the study. M.T. and T.A. performed the experiments and analyzed the data. All authors wrote the manuscript, made intellectual contributions, checked the interpretation of the results, and approved the final version of the manuscript.

Financial support

This work was funded by JSPS KAKENHI (Grant-in-Aid for Scientific Research C, grant numbers JP19K08809, JP21K08772) and by a HUSM Grant-in-Aid. The funders had no role in the study design, data collection, and analysis, decision to publish, or preparation of the manuscript.

Declaration of competing interest

T.O. received research funding for this study from Kyowa Kirin, Chugai Pharmaceutical, and TAIHO Pharmaceutical. However, the funders had no role in the study design, data collection and analysis, decision to publish, or preparation of the manuscript. The other authors indicated no potential conflicts of interest.

Acknowledgments

We are grateful to K. Hara and Y. Kinpara (Department of Pharmacology, Hamamatsu University School of Medicine) for maintaining the mouse colonies. We thank M. Kadohata, N. Anma (Third Division, Department of Internal Medicine, Hamamatsu University School of Medicine), R. Horiguchi, A. Kitamoto, M. Goda, Y. Inaba, N. Suzuki, and Y. Kawabata (Advanced Research Facilities and Services, Hamamatsu University School of Medicine) for providing their expertise and technical assistance. We also thank Editage (www.editage.jp) for the English language review.

Appendix A. Supplementary data

Supplementary data to this article can be found online at https://doi.org/10.1016/j.jphs.2022.04.009.

References

1. Kizaki M, Takahashi N, Iriyama N, et al. Efficacy and safety of tyrosine kinase inhibitors for newly diagnosed chronic-phase chronic myeloid leukemia over a 5-year period: results from the Japanese registry obtained by the New TARGET system. *Int J Hematol*. 2019;109:426–439. https://doi.org/10.1007/s12185-019-02613-1.
2. Bower H, Björkholm M, Dickman PW, et al. Life expectancy of patients with chronic myeloid leukemia approaches the life expectancy of the general population. *J Clin Oncol*. 2016;34:2851–2857. https://doi.org/10.1200/JCO.2015.66.2866.
3. Hochhaus A, Saglio G, Hughes TP, et al. Long-term benefits and risks of frontline nilotinib vs imatinib for chronic myeloid leukemia in chronic phase: 5-year update of the randomized ENESTnd trial. *Leukemia*. 2016;30:1044–1054. https://doi.org/10.1038/leu.2016.5.
4. Cortes JE, Saglio G, Kantarjian HM, et al. Final 5-year study results of DASISION: the dasatinib versus imatinib study in treatment-naïve chronic myeloid leukemia patients trial. *J Clin Oncol*. 2016;34:2333–2340. https://doi.org/10.1200/JCO.2015.64.8899.
5. Cortes JE, Kim DW, Pinilla-Ibarz J, et al. A phase 2 trial of ponatinib in Philadelphia chromosome-positive leukemias. *N Engl J Med*. 2013;369:1783–1796. https://doi.org/10.1056/NEJMoa1306494.
6. Valent P, Hadzijusufovic E, Schernthaner GH, et al. Vascular safety issues in CML patients treated with BCR/ABL1 kinase inhibitors. *Blood*. 2015;125:901–906. https://doi.org/10.1182/blood-2014-09-594432.
7. Dahlén T, Edgren G, Lambe M, et al. Cardiovascular events associated with use of tyrosine kinase inhibitors in chronic myeloid leukemia: a population-based cohort study. *Ann Intern Med*. 2016;165:161–166. https://doi.org/10.7326/M15-2306.
8. Aghel N, Delgado DH, Lipton JH. Cardiovascular events in chronic myeloid leukemia clinical trials. Is it time to reassess and report the events according to cardiology guidelines? *Leukemia*. 2018;32:2095–2104. https://doi.org/10.1038/s41375-018-0247-1.
9. Jain P, Kantarjian H, Boddu PC, et al. Analysis of cardiovascular and arteriothrombotic adverse events in chronic-phase CML patients after frontline TKIs. *Blood Adv*. 2019;3:851–861. https://doi.org/10.1182/bloodadvances.2018025874.
10. Fujioka I, Takaku T, Iriyama N, et al. Features of vascular adverse events in Japanese patients with chronic myeloid leukemia treated with tyrosine kinase inhibitors: a retrospective study of the CML Cooperative Study Group database. *Ann Hematol*. 2018;97:2081–2088. https://doi.org/10.1007/s00277-018-3412-8.
11. Valent P, Hadzijusufovic E, Hoermann G, et al. Risk factors and mechanisms contributing to TKI-induced vascular events in patients with CML. *Leuk Res*. 2017;59:47–54. https://doi.org/10.1016/j.leukres.2017.05.008.
12. Haguet H, Graux C, Mullier F, Dogné JM, Douxfils J. Long-term survival, vascular occlusive events and efficacy biomarkers of first-line treatment of CML: a meta-analysis. *Cancers*. 2020;12:1242. https://doi.org/10.3390/cancers12051242.
13. Steegmann JL, Cervantes F, le Coutre P, Porkka K, Saglio G. Off-target effects of BCR-ABL1 inhibitors and their potential long-term implications in patients with chronic myeloid leukemia. *Leuk Lymphoma*. 2012;53:2351–2361. https://doi.org/10.3109/10428194.2012.695779.
14. Sukegawa M, Wang X, Nishioka C, et al. The BCR/ABL tyrosine kinase inhibitor, nilotinib, stimulates expression of IL-1β in vascular endothelium in association with downregulation of miR-3p. *Leuk Res*. 2017;58:83–90. https://doi.org/10.1016/j.leukres.2017.05.005.
15. Ai N, Chong CM, Chen W, et al. Ponatinib exerts anti-angiogenic effects in the zebrafish and human umbilical vein endothelial cells via blocking VEGFR signaling pathway. *Oncotarget*. 2018;9:31958–31970. https://doi.org/10.18632/oncotarget.24110.
16. Durand MJ, Hader SN, Derayunan A, et al. BCR-ABL tyrosine kinase inhibitors promote pathological changes in dilator phenotype in the human microvasculature. *Microcirculation*. 2020;27:e12625. https://doi.org/10.1111/micc.12625.
17. Latifi Y, Moccetti F, Wu M, et al. Thrombotic microangiopathy as a cause of cardiovascular toxicity from the BCR-ABL1 tyrosine kinase inhibitor ponatinib. *Blood*. 2019;133:1597–1606. https://doi.org/10.1182/blood-2018-10-881557.
18. Hadzijusufovic E, Albrecht-Schgoer K, Huber K, et al. Nilotinib-induced vasculopathy: identification of vascular endothelial cells as a primary target site. *Leukemia*. 2017;31:2388–2397. https://doi.org/10.1038/leu.2017.245.
19. Pouwer MG, Pieterman EJ, Verschuren L, et al. The BCR-ABL1 inhibitors imatinib and ponatinib decrease plasma cholesterol and atherosclerosis, and nilotinib and ponatinib activate coagulation in a translational mouse model. *Front Cardiovasc Med*. 2018;5:55. https://doi.org/10.3389/fcvm.2018.00055.
20. Miyajima C, Iwaki T, Umemura K, Ploplis VA, Castellino FJ. Characterization of atherosclerosis formation in a murine model of type IIa human familial hypercholesterolemia. *BioMed Res Int*. 2018:1878964. https://doi.org/10.1155/2018/1878964.

21. Schneider CA, Rasband WS, Eliceiri KW. NIH Image to ImageJ: 25 years of image analysis. *Nat Methods*. 2012;9:671–675. https://doi.org/10.1038/nmeth.2089.
22. Cruz FF, Horta LF, Maia Lde A, et al. Dasatinib reduces lung inflammation and fibrosis in acute experimental silicosis. *PLoS One*. 2016;11, e0147005. https://doi.org/10.1371/journal.pone.0147005.
23. Zeng XP, Wang LJ, Guo HL, et al. Dasatinib ameliorates chronic pancreatitis induced by caerulein via anti-fibrotic and anti-inflammatory mechanism. *Pharmacol Res*. 2019;147:104357. https://doi.org/10.1016/j.phrs.2019.104357.
24. Schmidt V, Willnow TE. Protein sorting gone wrong–VPS10P domain receptors in cardiovascular and metabolic diseases. *Atherosclerosis*. 2016;245:194–199. https://doi.org/10.1016/j.atherosclerosis.2015.11.027.
25. Patel KM, Strong A, Tohyama J, et al. Macrophage sortilin promotes ldl uptake, foam cell formation, and atherosclerosis. *Circ Res*. 2015;116:789–796. https://doi.org/10.1161/CIRCRESAHA.116.305811.
26. Tveten K, Strøm TB, Cameron J, Berge KE, Leren TP. Mutations in the SORT1 gene are unlikely to cause autosomal dominant hypercholesterolemia. *Atherosclerosis*. 2012;225:370–375. https://doi.org/10.1016/j.atherosclerosis.2012.10.026.
27. Linsel-Nitschke P, Heeren J, Aherrahrou Z, et al. Genetic variation at chromosome 1p13.3 affects sortilin mRNA expression, cellular LDL-uptake and serum LDL levels which translates to the risk of coronary artery disease. *Atherosclerosis*. 2010;208:183–189. https://doi.org/10.1016/j.atherosclerosis.2009.06.034.
28. Kjolby M, Andersen OM, Breiderhoff T, et al. Sort1, encoded by the cardiovascular risk locus 1p13.3, is a regulator of hepatic lipoprotein export. *Cell Metabol*. 2010;8:213–223. https://doi.org/10.1016/j.cmet.2010.08.006.
29. Mortensen MB, Kjolby M, Gunnersen S, et al. Targeting sortilin in immune cells reduces proinflammatory cytokines and atherosclerosis. *J Clin Invest*. 2014;124:5317–5322. https://doi.org/10.1172/JCI76002.
30. Chen C, Li J, Matye DJ, Wang Y, Li T. Hepatocyte sortilin 1 knockout and treatment with a sortilin 1 inhibitor reduced plasma cholesterol in Western diet-fed mice. *J Lipid Res*. 2019;60:539–549. https://doi.org/10.1194/jlr.M089789.
31. Musunuru K, Strong A, Frank-Kamenetsky M, et al. From noncoding variant to phenotype via SORT1 at the 1p13 cholesterol locus. *Nature*. 2010;466:714–719. https://doi.org/10.1038/nature09266.
32. Moore KJ, Kunjathoor VV, Koehn SL, et al. Loss of receptor-mediated lipid uptake via scavenger receptor A or CD36 pathways does not ameliorate atherosclerosis in hyperlipidemic mice. *J Clin Invest*. 2005;115:2192–2201. https://doi.org/10.1172/JCI24061.